J Solid State Electrochem (2009) 13:1945–1949
DOI 10.1007/s10008-008-0741-x

ORIGINAL PAPER

# Characterization of $MoO_3$ nanorods for lithium battery using PVP as a surfactant

**Ch. V. Subba Reddy · Edwin H. Walker Jr. · S. A. Wicker Sr. · Quinton L. Williams · Rajamohan R. Kalluru**

Received: 9 September 2008 / Revised: 30 October 2008 / Accepted: 10 November 2008 / Published online: 4 December 2008


**Abstract** We synthesized $MoO_3$ nanorods using poly (vinyl pyrrolidone) (PVP) as a surfactant through the hydrothermal route for making a cathode for a lithium battery. Scanning electron microscopy images reveal the structures to have dimensions on the order of 1–10 μm in length and 50–200 nm in diameter. Analytical techniques such as X-ray diffractometry, Fourier transformation infrared spectroscopy, thermogravimetric analysis, and cyclic voltammetry were used to characterize the nanorods. The measured specific charge of $MoO_3$ nanorods prepared through a 15-day hydrothermal reaction was 156 $mAhg^{-1}$ during the initial discharge process.

**Keywords** Hydrothermal method · Nanorods · Surfactant · Lithium battery

## Introduction

Many transition metal oxides have been investigated for possible use as active materials in electrodes for secondary lithium batteries [1]. Some of the transition metal oxides have been tested as positive electrodes based on toxicity, performance, and cost. The molybdenum oxides ($MoO_3$) have received great attention due to their physical and chemical properties within the group of transition metal oxides [2]. Various nanostructures of $MoO_3$ such as nanobelts, nanowires, nanorods, and nanotubes have been synthesized using a variety of methods, such as hydrothermal treatment, sol–gel process, and chemical vapor deposition [2–4]. Nanostructured $MoO_3$ have potential applications for lithium batteries [2], smart windows, catalysts, sensors, and electrochromic devices [5–8].

In the continuing pursuit of preparing organic–inorganic nanocomposites with superior properties, the inclusion of conducting polymers in layered hosts and other structurally organized environments is a topic of substantial interest. Resulting hybrid nanostructures have the potential of holding novel structural, mechanical, and electrical properties [9]. Recently, we have prepared the ($MoO_3$+PVP+PVA) nanocomposite and its application as an electrode material for secondary lithium battery [10]. In this system, we found better cycle stability and lower capacity of the ($MoO_3$+PVP+PVA) used as a cathode for lithium battery compared to the $MoO_3$ cathode. However, the morphology of the ($MoO_3$+PVP + PVA) material changed from nanobelts to nanoparticles. To examine the change of morphology, we report the time-dependent hydrothermal synthesis of $MoO_3$ nanorods using only PVP as a surfactant.

## Experimental

The surfactant-free and $MoO_3$ surfactant(PVP) used 4 and 15 days hydrothermal-treated $MoO_3$ nanorods were synthesized from their solutions. $MoO_3 \cdot nH_2O$ sols were prepared by ion exchange of ammonium heptamolybdate tetrahydrate $(NH_4)_6Mo_7O_{24} \cdot 4H_2O$ (≥99.0%) through a

C. V. Subba Reddy (✉) · E. H. Walker Jr. · S. A. Wicker Sr.
Department of Chemistry,
Southern University and A&M College,
P.O. Box 12566, Baton Rouge, LA 70813, USA
e-mail: drsreddy2005@yahoo.com

Q. L. Williams · R. R. Kalluru
Department of Physics, Atmospheric Sciences and Geoscience,
Jackson State University,
JSU Box. 17660, 1400 J.R. Lynch Street,
Jackson, MS 39217, USA

R. R. Kalluru
e-mail: rajamohan.r.kalluru@jsums.edu

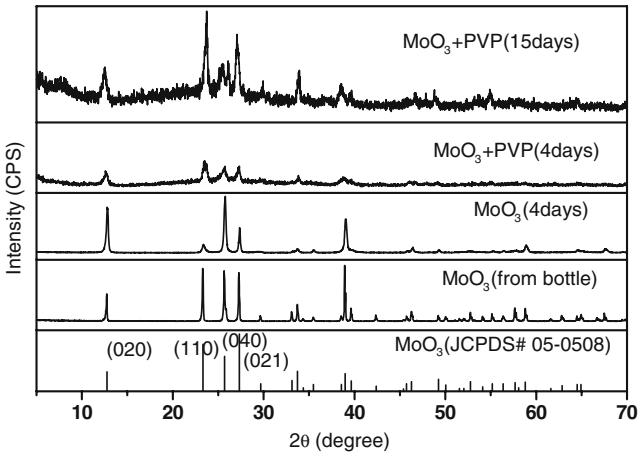


**Fig. 1** XRD patterns of the surfactant used $MoO_3$ nanorods

proton exchange resin. After ion exchange, a clear light-blue $MoO_3$ sol (pH ~ 2.0) was obtained and modified with poly(vinyl pyrrolidone) (PVP). The molar ratio of PVP to $MoO_3$ sol was 0.5. The modified solutions were stirred for 12 h at room temperature and then poured into a Teflon-lined autoclave and kept at 180 °C for 4 and 15 days in an oven. After the hydrothermal reaction, the light blue product was washed with distilled water and dried at 80 °C for 10 h.

Crystallographic information of the samples was investigated with a Bruker D8 Advance X-ray powder diffraction (XRD) spectrometer employed with graphite monochromatized Cu K$\alpha$ radiation ($\lambda$=1.54187 Å). The diffraction data were collected over the 2$\theta$ range from 5° to 70°. Fourier transform infrared (FTIR) absorption spectra of the nanobelts were recorded using a 60-SXB IR spectrometer of 4 $cm^{-1}$ resolution, over a wavenumber range of 400–4,000 $cm^{-1}$. The thermal stability of the samples was studied using thermogravimetric analysis (TGA). The samples were heated from room temperature to 600 °C at a rate of 10 °C $min^{-1}$ on a TA 600 instrument. Raman spectra were taken under ambient condition by using Renishaw inVia Raman microscope excited with a 514-nm $Ar^+$ laser. Raman Spectra were taken with 98.5% accuracy. The morphologies of the resulting products were characterized using a scanning electron microscope (SEM; JSM 6390). Cyclic voltammetric (CV) properties of the nanorods were investigated with a three-electrode cell with a platinum counter electrode and a silver (Ag) wire reference electrode. The working electrode, prepared by mixing 75 wt.% of active material, 20 wt.% of carbon black, and 5 wt.% of ethylene cellulose, was then coated on a 1.5-$cm^2$ ITO glass. A solution of 1 M lithium perchlorate in propylene carbonate was used as the electrolyte, after purification by recrystallization of lithium perchlorate (99.99%, Aldrich) and by distillation of propylene carbonate (99.7%, Aldrich), respectively. Cyclic voltammetric (CV) measurements were carried out between the potential limits of −1.5 and +0.5 V versus a Ag reference electrode using a potentiostat/galvanostat (Zahner IM6). The CV curves were recorded at a scan rate of 10 mV/s.

The electrochemical property of surfactant-free $MoO_3$ and surfactant-used 15 days hydrothermal-treated $MoO_3$ nanorods was measured with a multichannel galvanostat/potentiostat system (MacPilew with 99% accuracy) by applying a constant current (0.4 mA/$cm^2$) in the potential range of 4.0–1.5 V. Electrochemical cells were prepared using a lithium pellet as the negative electrode, a 1-mol $dm^{-3}$ solution of $LiPF_6$ in ethylene carbonate (EC)/dimethyl carbonate (DMC) as an electrolyte, a pellet made of the nanorods, acetylene black, and PTFE in a 75:20:05 weight ratio as a positive electrode.

## Results and discussion

The XRD pattern of $MoO_3$ nanorods is shown in Fig. 1. All the peaks are indexed to $\alpha$-$MoO_3$ [JCPDS card No. 05-0508] with lattice constants $a$=3.962 Å, $b$=13.858 Å, and $c$=3.697 Å. The strong diffraction peaks of (020), (040), and (060) planes reveal a layered crystal structure or a highly anisotropic growth of the oxides [2]. The surfactant-used 4 and 15 days hydrothermal-treated $MoO_3$ nanorods are shown in Fig. 1. In the surfactant-used $MoO_3$ nanorods, we observed a decrease in the (020) peak intensity and an increment in the FWHM of the peak and (110), (021) peak intensities are increased for 15-days hydrothermal-treated nanorods.

FTIR patterns of surfactant-free $MoO_3$ and the surfactant used 15-days hydrothermal-reacted $MoO_3$ nanorods are shown in Fig. 2. In the case of surfactant-free $MoO_3$ nanorods, the band at 1,000 $cm^{-1}$ can be assigned to the stretching mode of Mo-terminal oxygen, and bands at 872

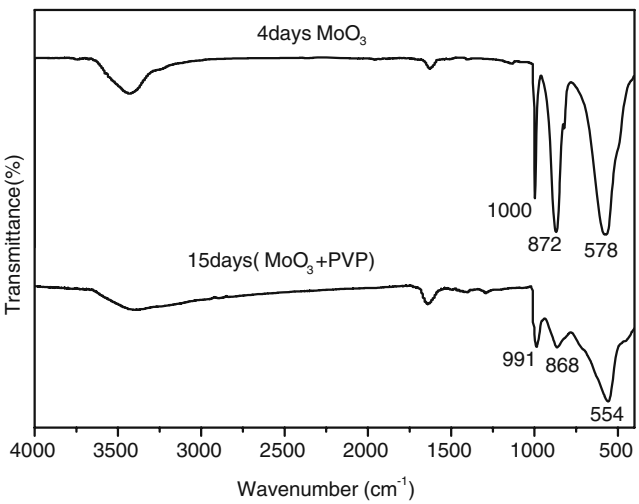


**Fig. 2** FTIR spectra of the surfactant used $MoO_3$ nanorods

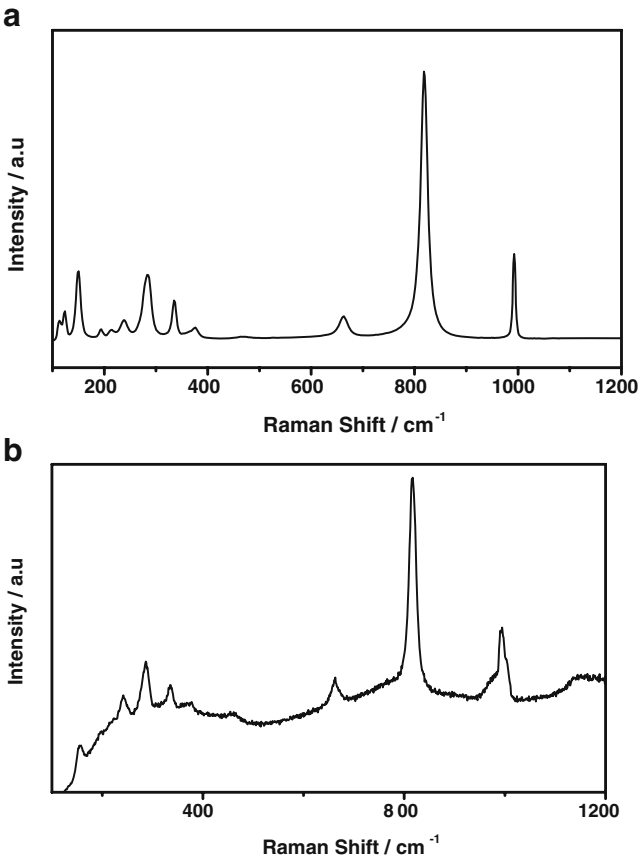


**Fig. 3** Raman spectra of the **a** $MoO_3$ nanorods, **b** surfactant used $MoO_3$ nanorods

and 578 $cm^{-1}$ can be assigned to the stretching vibrations of the O(3) and O(2) atoms linked to two or three Mo atoms, respectively [11]. The positions of all three bands are shifted toward the lower wavenumbers side in the surfactant used 15 days hydrothermal reacted $MoO_3$ nanorods due to increasing of the layer distance in $MoO_3$.

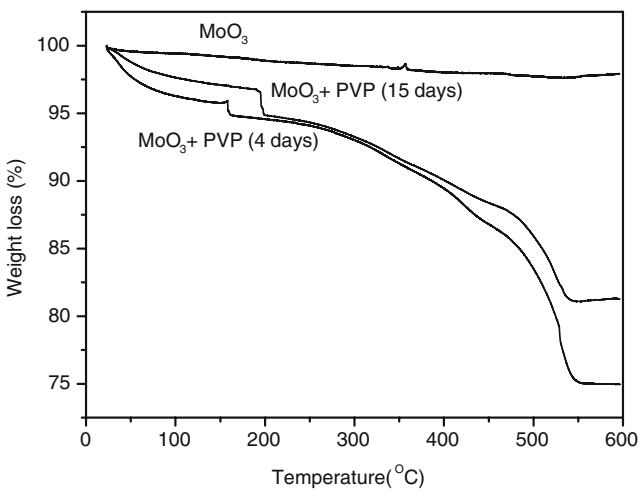


**Fig. 4** TGA curves of the surfactant used $MoO_3$ nanorods

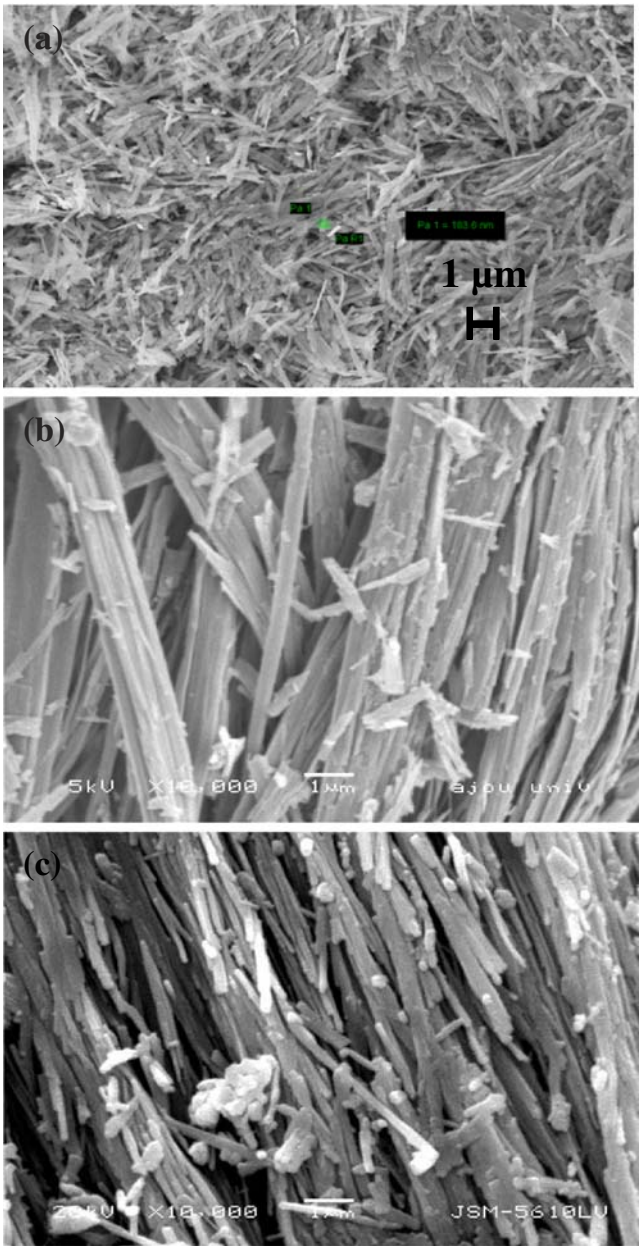


**Fig. 5** SEM images of (**a**) $MoO_3$, (**b**) $MoO_3$+PVP(4 days), (**c**) $MoO_3$+PVP (15 days) nanorods

Raman spectroscopy was used to characterize the orthorhombic $MoO_3$ structure through weak Raman signals at 664 and 820 $cm^{-1}$ corresponding to the stretching modes $\nu$(O-Mo-O; Fig. 3a). The Raman peaks of the surfactant-used 15-days hydrothermal-reacted $MoO_3$ nanorods (Fig. 3b) shifted toward lower wavenumbers. The most notable change of the bending mode $\delta$ (O-Mo-O) was in the range of 120 to 220 $cm^{-1}$. Both FTIR and Raman spectra confirm that the stretching modes shift toward the lower wavenumbers when PVP was used as a surfactant to prepare $MoO_3$ nanorods.

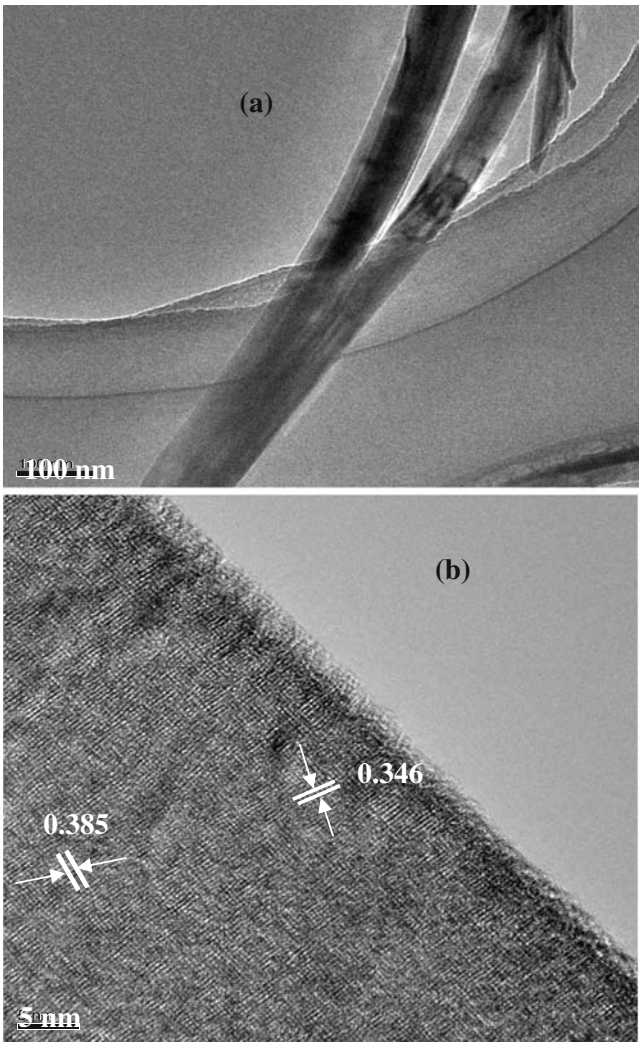


**Fig. 6** (**a**) TEM image of $MoO_3$+PVP(15 days) nanorod, (**b**) HRTEM image of $MoO_3$+PVP(15 days) nanorod

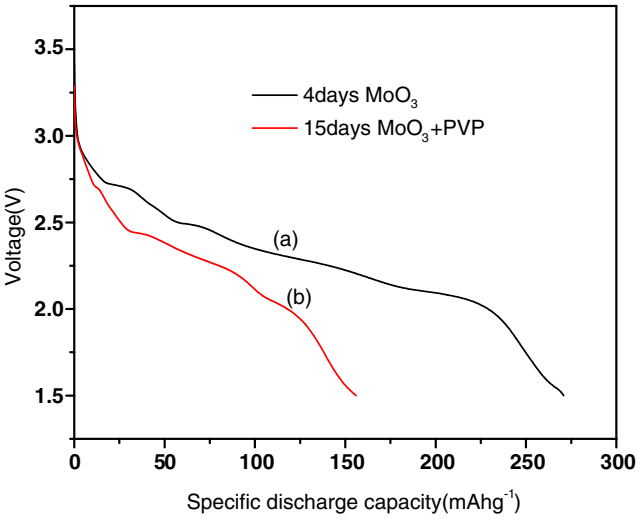


**Fig. 8** Initial discharge curves of lithium battery (**a**) $MoO_3$ nanorods, (**b**) $MoO_3$+PVP (15 days) nanorods

Thermal stability of the surfactant-free and $MoO_3$ surfactant-used 4 and 15 days hydrothermal-treated $MoO_3$ nanorods is shown in Fig. 4. $MoO_3$ nanorods exhibits <0.5% weight loss, indicating the completeness of the decomposition of the $MoO_3$ sol during the hydrothermal treatment at 180 °C. Two weight loss curves are observed in surfactant-used 4 and 15 days hydrothermal-treated $MoO_3$ nanorods. The first weight loss corresponds to the release of water and the second one to the decomposition of surfactant.

SEM photographs of the surfactant-free and $MoO_3$ surfactant-used 4 and 15 days hydrothermal-reacted $MoO_3$ nanorods are shown in Fig. 5. Figure 5a shows individual nanorods with diameters ranging from 10 to 100 nm and length 1–5 μm. Figure 5b shows the surfactant-used 4 days hydrothermal-reacted $MoO_3$ nanorods with the width of

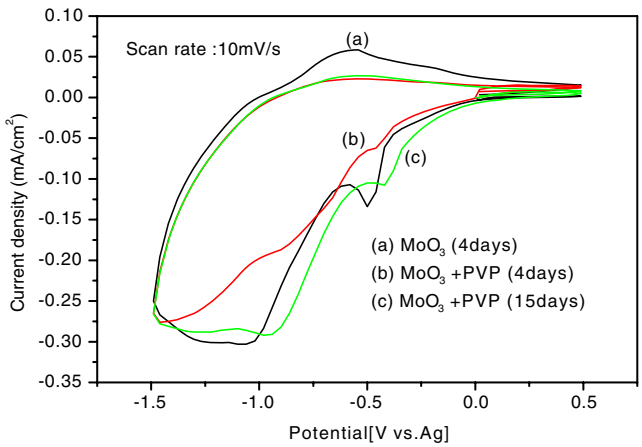


**Fig. 7** Cyclic voltammograms (CVs) curves of the surfactant used $MoO_3$ nanorods

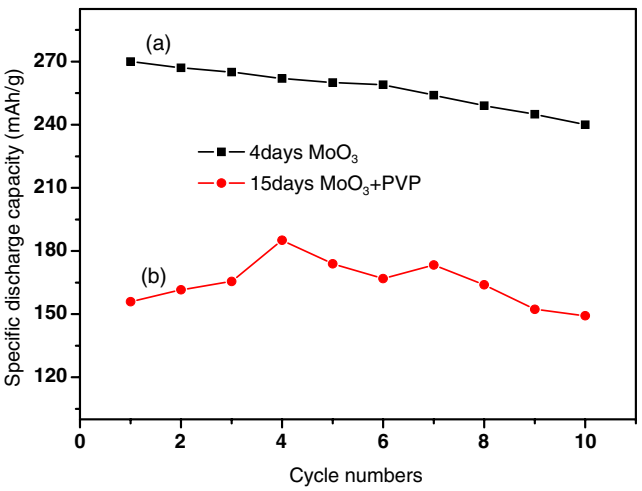


**Fig. 9** Cyclic property of lithium battery (**a**) $MoO_3$ nanorods, (**b**) $MoO_3$+PVP (15 days) nanorods

100 nm and several micrometers in length. The surfactant used 15 days hydrothermal-reacted $MoO_3$ nanorods (Fig. 5c) well crystallized and grew longer with a typical length of 6 μm and diameter ranging from 5 to 100 nm. The sample prepared without PVP was very similar to the nanofibers with different diameters along the *b*-axis, and the side faces of the products were not smooth. Figure 5b, c shows that, in PVP used samples, assembled nanorods were obtained with uniform diameter and smooth lateral surfaces. The addition of PVP is a vital factor in the morphology. In the $MoO_3$/PVP systems, the PVP acts as a template surfactant in forming a chain structure. The $MoO_3$ may rise up along the chains to form $MoO_3$ nanorods. On the other hand, the PVP forms a shell surrounding the particles to avoid them from grain growth as a consequence of its steric effect. As a result, monodispersed $MoO_3$ nonorods were finally obtained [12, 13].

TEM image of 15 days hydrothermal-treated $MoO_3$ single nanorod is shown in Fig. 6a. Figure 6b shows a high-resolution transition electron microscopy (HRTEM) image with two sets of parallel fringes, normal to each other, and with the spacing of 0.385 and 0.346 nm, corresponding to (110) and (040) planes of orthorhombic structure $MoO_3$.

The cyclic voltammograms (CVs) of the $MoO_3$ nanorods and surfactant-used 4 and 15 days hydrothermal-treated $MoO_3$ nanorods are shown in Fig. 7. The CVs of $MoO_3$ nanorods and surfactant-used 4 and 15 days hydrothermal-treated $MoO_3$ nanorods exhibit two broad cathodic bands at −0.5 and −1.04, −0.45 and −0.87, −0.94 and −0.41 V and one broad anodic band at −0.57, −0.53, and –0.62 V, respectively, which are attributed to the lithium ion insertion to and exclusion from the $MoO_3$ nanorod electrode materials.

The first discharge curve for the surfactant-free $MoO_3$, the surfactant-used 15 days hydrothermal-treated $MoO_3$ nanorods are shown in Fig. 8. The discharge capacity of the surfactant-used 15 days hydrothermal-treated $MoO_3$ nanorods battery (158 $mAhg^{-1}$ in the potential range of 3.45 to 1.5 V) is lower than that of the surfactant-free $MoO_3$ nanorod batteries (270 $mAhg^{-1}$ in the potential range of 3.25 to 1.5 V). The decreased capacity in the surfactant-used 15 days hydrothermal-treated $MoO_3$ nanorods battery might be due to a decreased average molybdenum oxidation state or due to the amorphous nature of cathode materials [10].

Figure 9 shows the charge–discharge cycles of the surfactant-free $MoO_3$ and the surfactant-used 15 days hydrothermal-treated $MoO_3$ nanorods batteries for ten cycles. The specific discharge capacity of the surfactant-free $MoO_3$ battery after ten cycles was 240 $mAhg^{-1}$, and the cell exhibited a capacity loss of 11%, demonstrating good cycle stability. The specific discharge capacity of the surfactant-used 15 days hydrothermal-treated $MoO_3$ nanorods battery after ten cycles was 149 $mAhg^{-1}$ and capacity loss was 5%.

## Conclusion

The surfactant-free and the surfactant-used, 4 and 15 days hydrothermal-treated $MoO_3$ nanorods were successfully synthesized by hydrothermal process. The electrochemical measurements show that the surfactant-free $MoO_3$ nanorods have higher specific charge capacity than the surfactant-used, 15 days hydrothermal-treated $MoO_3$ nanorods.

**Acknowledgments** This research was made possible by grants supplied by the National Science Foundation's Early CAREER program (cooperative agreement DMR-0449886) at Southern University. The purchase of the X-ray powder diffractometer was made possible by grant no. LEQSF(2006-2008)-ENH-TR-68, the purchase of the FTIR was made possible by grant no. LEQSF(2005-2007)-ENH-TR-65, as well as the purchase of the SEM was made possible by grant no. LEQSF(2007-2009)-ENH-TR-68, administered by the Louisiana Board of Regents. This research was made possible by a grant supplied by the U.S. Dept. of Education Title III Part B HBGI program (Grant No. P031B040030) at Southern University.

## References

1. Ceder G, Chiang YM, Sadoway DR, Aydinol MK, Jang YI, Huang B (1998) Nature 392:694. doi:10.1038/33647
2. Mai L, Hu B, Chen W, Qi Y, Lao C, Yang R, Dai Y (2007) Adv Mater 19:3712. doi:10.1002/adma.200700883
3. Mai LQ, Chen W, Xu Q, Zhu QY (2003) Micro Engg 66:199
4. Sobia A, Christopher SB, Geoffrey H, Ivan PP (2006) J Mater Chem 16:3575. doi:10.1039/b607335b
5. Lou XW, Zeng HC (2002) Chem Mater 14:4781. doi:10.1021/cm0206237
6. Zhou J, Xu NS, Deng SZ, Chen J, She JC, Wang ZL (2003) Adv Mater 15:1835. doi:10.1002/adma.200305528
7. Li XL, Liu JF, Li YD (2002) Appl Phys Lett 81:4832. doi:10.1063/1.1529307
8. Somani PR, Radhakrishnan S (2002) Mater Chem Phys 77:117. doi:10.1016/S0254-0584(01)00575-2
9. Gomez-Romero P (2001) Adv Mater 13:163. doi:10.1002/1521-4095(200102)13:3<163::AID-ADMA163>3.0.CO;2-U
10. Subba Reddy Ch V, Qi YY, Jin W, Zhu QY, Deng ZR, Chen W, Mho SI (2007) J Solid State Electrochem 11:1239. doi:10.1007/s10008-007-0278-4
11. Dong W, Dunn B (1998) J Non-Cryst Solids 225:135. doi:10.1016/S0022-3093(98)00018-0
12. Qingqing W, Gaoling Z, Gaorong H (2005) Mater Lett 59:2625. doi:10.1016/j.matlet.2005.04.004
13. Bai F, He P, Jia Z, Huang X, He Y (2005) Mater Lett 59:1687. doi:10.1016/j.matlet.2005.01.039